

# Computational study of enantioselective interaction between C<sub>60</sub> fullerene and its derivatives with L-histidine

Bhajan Lal

Received: 6 August 2006 / Accepted: 26 January 2007 / Published online: 23 February 2007  
© Springer-Verlag 2007

**Abstract** The mechanism of the enantioselective binding of L-histidine with C<sub>60</sub> fullerene and its derivatives, (1,2-methanofullerene C<sub>60</sub>)-61-carboxylic acid, diethyl (1,2-methanofullerene C<sub>60</sub>)-61-61-dicarboxylate and tert-butyl (1,2-methanofullerene C<sub>60</sub>)-61-carboxylate based chiral selectors was studied by quantum chemical calculations. All the molecules were fully optimized at RHF/6-31G\* basis set. Relative energies between the different complexes were subsequently estimated with single-point electronic energies computed using Møller-Plesset perturbation theory (MP2). Stability and feasibility of all the generated structures were supported by their respective energy minima and fundamental frequencies. It was observed that interaction of fullerene derivatives with L-histidine is due to the existence of hydrogen bonding forces during the complex formation. The intermolecular forces, flow of atomic charges, binding energy, hardness, dipole moment and localization of electrostatic potential are in agreement with enantioselective interaction of L-histidine with C<sub>60</sub> fullerene and its derivatives. It is found that theoretical evaluation to be consistent with the experimental data.

**Keywords** Chiral recognition interaction · C<sub>60</sub> Fullerene derivatives · Fundamental frequencies · L-histidine · Møller-Plesset perturbation theory

## Introduction

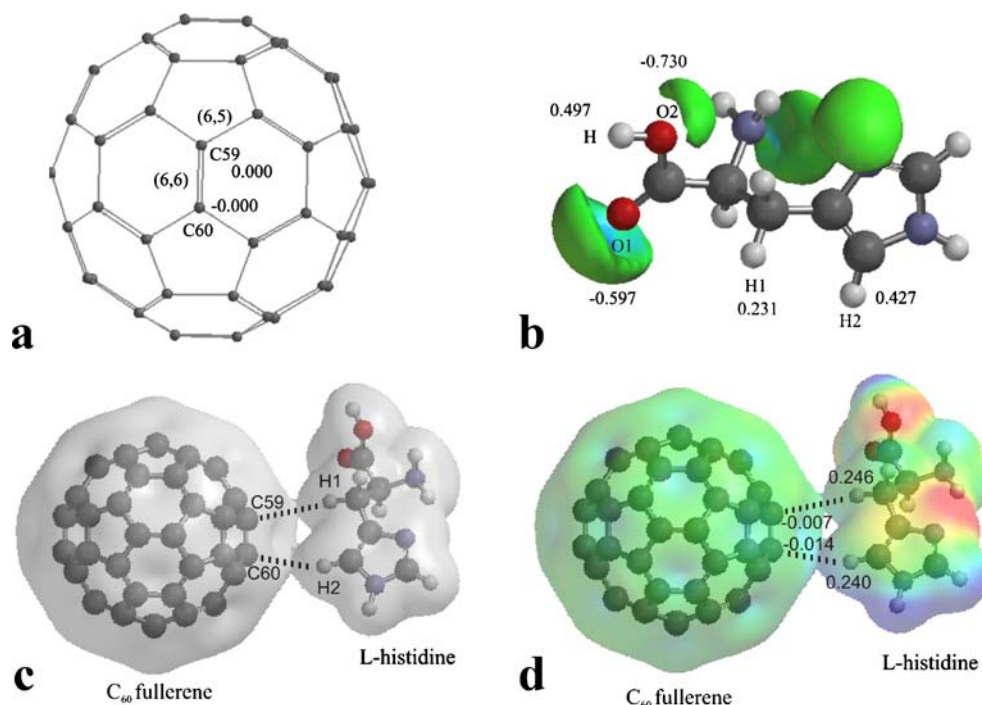
Chiral recognition, as an aspect of molecular recognition, has been a subject of great interest because the majority of bioorganic molecules are chiral and the behaviour of enantiomers in a chiral environment is different [1]. It implies a set of weak forces of interactions ranging from hydrogen bonding to van der Waals interactions through ionic and dipole-dipole interactions [2]. Various types of intermolecular forces have been extensively studied and well documented [3]. In some cases the weak intermolecular forces are most discriminating, while in other cases the strong hydrogen bonding forces are most responsible, enantiodiscriminating forces are thus case dependent. Precisely how intermolecular forces act, in concert, to discriminate between enantiomers is not well established.

An important feature of fullerene molecules is that they have numerous points of attachment, allowing for precise grafting of active chemical groups in three-dimensional orientations [4]. This attribute, the hallmark of rational drug design, allows positional control in matching fullerene compounds to biological targets [5]. Studies towards yielding valuable viable fullerene-based products, have demonstrated beneficial in vitro biological applications for C<sub>60</sub> and its organic-functionalized derivatives [6–11]. Recent studies show that the fullerene carbon cage is relatively non-toxic and not metabolized in vivo [12]. Wilson et al. identified and modeled the probable binding site for C<sub>60</sub> fullerene and discuss the interatomic interactions that stabilize the antibody-fullerene complex [13]. Recently, it has been reported that the shape of C<sub>60</sub> fullerene enhances the selectivity and enantioselectivity of their interaction with a specific enantiomer [14].

From the theoretical point of view, electronic structure studies have been mainly carried out for magic number

B. Lal (✉)  
Department of Chemistry, Bioanalytical Laboratory,  
University of Pretoria,  
Pretoria 0002, South Africa  
e-mail: bhajanks@hotmail.com

**Fig. 1** Molecular structures by computations: **a**  $C_{60}$  fullerene showing two binding types (6,5) and (6,6); **b** electrostatic potential map of L-histidine, selected atomic charges are labelled; **c** electron density of complex formed between  $C_{60}$  fullerene and L-histidine, showing overall size and shape of the molecules during intermolecular interaction; **d** density encoded with electrostatic potential of the complex formed between  $C_{60}$  fullerene and L-histidine, some selected atomic charges are labelled, red is the electronegative region and blue is the electropositive region



fullerene where, in general, the high symmetry of these structures is of great help to perform calculations [15]. It has been well studied by possible existing computational methods such as *ab initio* and Density function theory, [16] semi-empirical [17]. Several research groups have published papers on novel physico-chemical properties of buckyball [18]. Owing to high polarizability, large size and electronic effect,  $C_{60}$  fullerenes forms a lot of molecular complex [19, 20].

L-Histidine is one of the essential amino acids. It has been shown that an indispensable amino acid, L-histidine, which is a precursor of histamine, possesses anticonvulsant activity in several seizure models and can be a beneficial adjuvant for anticonvulsive therapy [21]. A fine scaly erythematous dermatitis is developed for patients on long-term total

parental nutrition if no histidine is included in the intravenous nutrient solution [22]. It is necessary for L-histidine to be considered to be at least partially a dietary essential even though L-histidine is not nutritionally important.

It has been reported previously [23] that the fullerene and its derivatives which showed enantioselective response characteristics, successfully determinate the enantiopurity of L-histidine as raw material and of its pharmaceutical formulations. This report is a further step dealing with the computational study directed towards the understanding of intermolecular forces of interactions take place between L-his and  $C_{60}$  fullerene or its derivatives. Indeed, structural elucidation and physicochemical properties of all the molecules involved in this study could be beneficial for the drug design and pharmacological utility.

**Fig. 2** Distances obtained from computational calculations of complexes: **a**  $C_{60}$  fullerene with L-histidine; **b** (1,2-methanofullerene  $C_{60}$ )-61-carboxylic acid with L-histidine; **c** diethyl (1,2-methanofullerene  $C_{60}$ )-61-61-dicarboxylate with L-histidine 8; **d** tert-butyl (1,2-methanofullerene  $C_{60}$ )-61-carboxylate with L-histidine 9

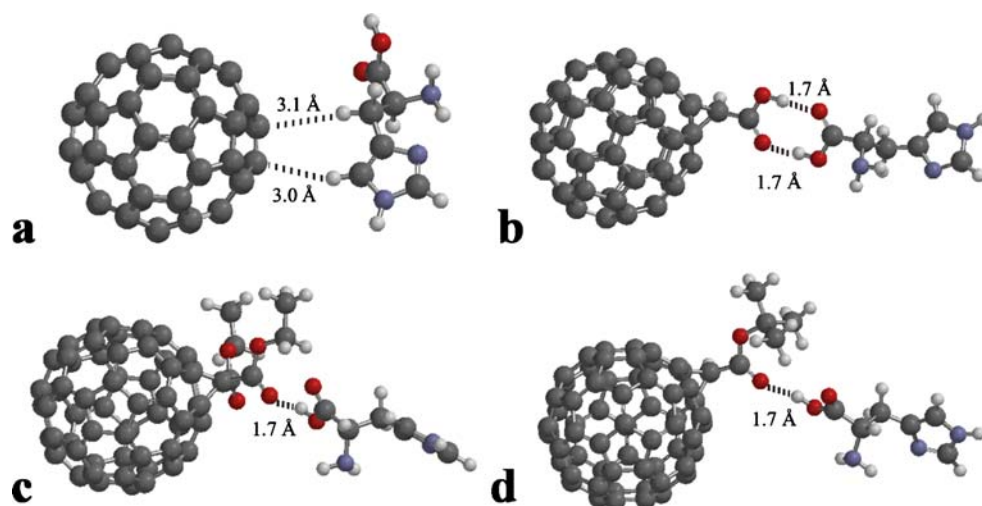
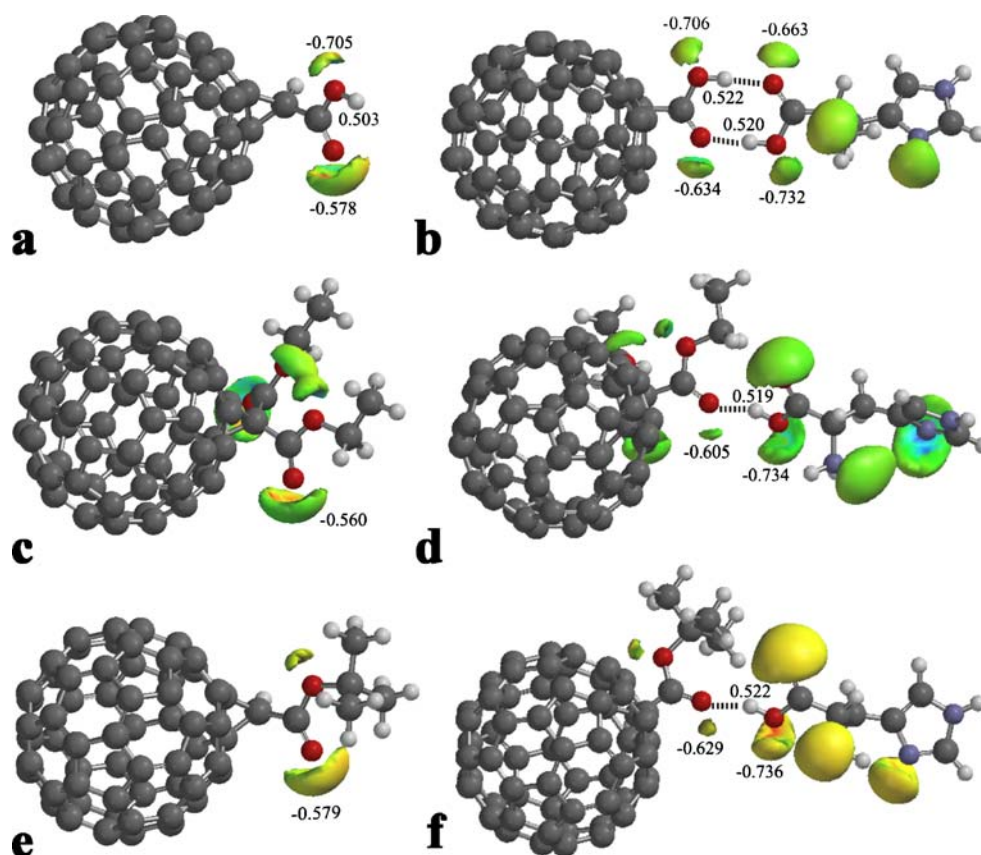


**Fig. 3** Electrostatic potential map and selected atomic charges: **a** (1,2-methanofullerene  $C_{60}$ )-61-carboxylic acid; **b** complex between (1,2-methanofullerene  $C_{60}$ )-61-carboxylic acid and L-histidine, showing intermolecular interaction; **c** diethyl (1,2-methanofullerene  $C_{60}$ )-61-61-dicarboxylate; **d** complex between diethyl (1,2-methanofullerene  $C_{60}$ )-61-61-dicarboxylate and L-histidine showing intermolecular interaction; **e** tert-butyl (1,2-methanofullerene  $C_{60}$ )-61-carboxylate; **f** complex between tert-butyl (1,2-methanofullerene  $C_{60}$ )-61-carboxylate and L-histidine showing intermolecular interaction



## Methods

The molecular structures of  $C_{60}$  fullerene (1), (1,2-methanofullerene  $C_{60}$ )-61-carboxylic acid (2), diethyl (1,2-methanofullerene  $C_{60}$ )-61-61-dicarboxylate (3), tert-butyl (1,2-methanofullerene  $C_{60}$ )-61-carboxylate (4), L-histidine (L-his) (5), complex between  $C_{60}$  and L-his (6), complex between (1,2-methanofullerene  $C_{60}$ )-61-carboxylic acid and L-his (7), complex between diethyl (1,2-methanofullerene  $C_{60}$ )-61-61-dicarboxylate and L-his (8), and complex between tert-butyl (1,2-methanofullerene  $C_{60}$ )-61-carboxylate and L-his (9), were generated for the prediction of interaction between fullerene and its derivatives with L-histidine.

The electronic structures with lower energy conformation and derived physicochemical properties of all the compounds 1 to 9 were obtained by *ab initio* theory. However, molecular calculations started with the fully

optimized semiempirical PM3 level of theory, followed by the minimal STO-3G basic set Hartree-Fock model. The resulting wavefunction, Hessian matrix and the geometry of the molecules obtained were used to perform the next calculation with the split-valence basis set 3-21G(\*). The procedure was applied further for next calculation at HF/6-31G\* level. Relative energies between the different complexes were estimated with single-point electronic energies computed using wavefunctions incorporating electron correlation through Møller-Plesset perturbation theory (MP2). Asterisk means that “d” polarization functions were added for carbon, oxygen and nitrogen atoms.

To obtain the real and detain picture of intermolecular interaction, the following physicochemical parameters were explored: total energy, highest occupied MO (HOMO), lowest unoccupied MO (LUMO), intermolecular distances, atomic charges, electrostatic potential, bond length, hard-

**Table 1** Calculated most representative bond lengths of fullerene and its derivatives separately and with L-histidine as complexes

Bond	Molecules							
	1	6	2	7	3	8	4	9
(6,6)	1.378	1.369	1.552	1.553	1.592	1.549	1.550	1.551
(6,5)	1.464	1.455	1.497	1.498	1.488	1.499	1.496	1.495

Bond lengths calculated in Ångstroms

ness ( $\eta$ ) and dipole moment ( $\mu$ ). Fundamental frequencies at the semiempirical level (PM3) of all the molecules were calculated and assigned as minima (all real frequencies). The software utilized was Spartan'04 Windows [24] and CorelDRAW 12.

## Results and discussion

It has been reported experimentally [23] that  $C_{60}$  fullerene and its derivatives electrodes are simple, fast and reproducible, low cost and reliable for the enantioanalysis of L-histidine. The present report gives more detail on how the intermolecular forces act between L-histidine and  $C_{60}$  fullerene 1 or its derivatives 2, 3 and 4. The lower energy electronic structures of 1, 2, 3, 4 and 5 molecules and 6, 7, 8 and 9 complexes were calculated.

The theoretical results revealed that RHF/6-31\* calculations are satisfactory for optimizing the geometry of complexes. However, they show inability to satisfactorily take into account electron correlation and, therefore, dispersion, which has its origin in molecular polarization and electron correlation would be in principal required for such a study. Thus relative energies between the different complexes were subsequently estimated with single-point electronic energies computed using wavefunctions incorporating electron correlation through Moller-Plesset perturbation theory (MP2).

Electronic structures of all the molecules and complexes are presented in Figs. 1, 2 and 3. The fullerene X-ray structure [25] shows two different bond lengths (1.389 Å and 1.432 Å) for the bond between two hexagons and for those between a hexagon and a pentagon, referred as (6,6) and (6,5), respectively, as shown in Fig. 1a. Both numbers lie between standard  $sp^2$ - $sp^2$  (1.33 Å) and  $sp^3$ - $sp^3$  (1.54 Å) bond lengths. Table 1 displays the most representative bond lengths (6,6) and (6,5), obtained in these computations. It is worthwhile to mention here that computed bond lengths

**Table 2** Values of the physicochemical properties of all the compounds

Compound	Energy <sup>a</sup>	HOMO-1 <sup>b</sup>	HOMO <sup>b</sup>	LUMO <sup>b</sup>	LUMO+1 <sup>b</sup>
1	-2271.82123	-6.05	-6.04	-3.09	-3.07
2	-2499.67768	-5.69	-5.82	-3.16	-3.07
3	-2845.48755	-5.93	-5.79	-3.11	-3.04
4	-2656.94640	-5.91	-5.76	-3.15	-3.01
5	-547.123755	-9.06	-5.80	0.39	5.45
6	-2819.56811	-6.11	-5.97	-2.77	-2.70
7	-3048.43321	-5.89	-5.74	-3.02	-3.00
8	-3394.26248	-5.84	-5.82	-3.12	-3.08
9	-3205.69927	-5.85	-5.75	-3.09	-3.01

<sup>a</sup> Hartrees, <sup>b</sup> electron Volts (eV)

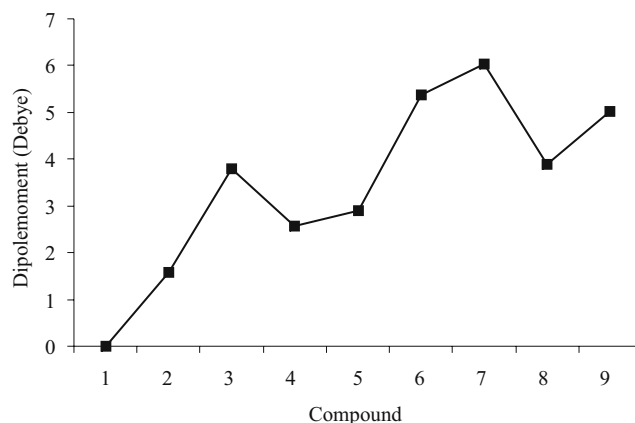


**Fig. 4** Dipole moment profile for the molecular interaction between  $C_{60}$  fullerene and its derivatives with L-histidine

always reasonably reproduce some experimental differences. In significant manner, the (6,6) bond length ( $C_{59}$ – $C_{60}$ ) of fullerene derivatives 2, 3, 4 and of their complexes 7, 8 and 9 show the single bond character due to the presence of bridging  $C_{61}$  carbon atom with fullerene cage, which changes the corresponding  $sp^2$ - $sp^2$  bond character of (6,6) bond of ( $C_{59}$ – $C_{60}$ ) to  $sp^3$ - $sp^3$  bond. Accordingly, the bond lengths are in favour of the accuracy of the geometry and symmetry of the  $C_{60}$  fullerene and its derivatives obtained from theoretical investigation.

The distances from carbon atoms of  $C_{60}$  fullerene to hydrogen atoms of L-his in complex 6 were found as 3.1 Å and 3.0 Å, respectively, which exhibit a very weak interaction between hydrogen atoms of L-his amino acid and  $\pi$  electrons of the fullerene cage. Intermolecular distances of interaction involved in all the complexes are presented in Fig. 2. Hydrogen-bonding distances (1.7 Å) were found in complexes 7, 8 and 9, which are responsible for selectivity and enantioselectivity. The complex 7 has two hydrogen bonding distance which is between two carboxylic groups as shown in Fig. 2b. In 8 and 9, hydrogen bonding is between carboxylate oxygen of fullerene derivatives and carboxylic hydrogen of L-histidine. It is concluded that the fullerene derivative 2 shows significant interaction with L-his than fullerenes 1, 3, 4, as indicated by the two hydrogen bonding distances in the former as demonstrated in Fig. 2b. It is in good agreement with the EPME experiment [23] since the slope of the electrode 2 has been obtained as 57.71, follows the ideal Nernst equation and thus reported as the best responding electrode.

Some molecular properties changed from structure 1 ( $C_{60}$  fullerene) to 6 (complex between  $C_{60}$  and L-his) as a consequence of different electronic distribution. As revealed from Fig. 1a, carbon atoms  $C_{59}$  and  $C_{60}$  of molecule 1 increased their electronegativity, when compared with complex 6 (Fig. 1d). Thus, the interaction of  $C_{60}$

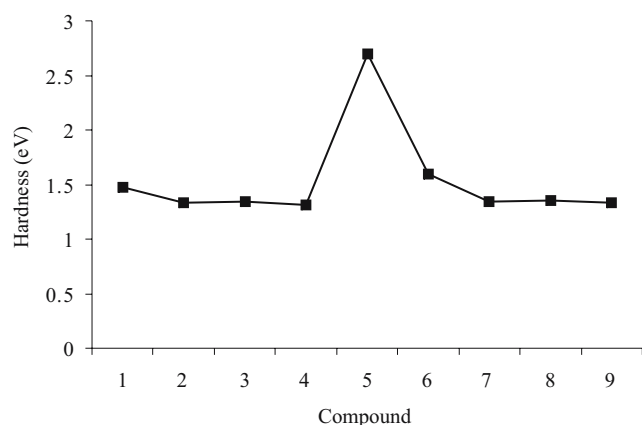


**Fig. 5** Hardness profile for the molecular interaction between  $C_{60}$  fullerene and its derivatives with L-histidine

with L-his is in agreement with the changes in atomic charges as the polarization of C atoms from molecule 1 (Fig. 1a) to complex 6 (Fig. 1d) signify that C atoms could share charges with H1 and H2 atoms of L-his. As a result, hydrogen atoms H1 and H2 show the increase and decrease in electropositivity, respectively, when compared Fig. 1b with Fig. 1d. Atomic charges calculated in electrons.

It is observed that oxygen and hydrogen atoms increased their electronegativity and electropositivity, respectively, from fullerene derivatives 2, 3, and 4 (Fig. 3a,c,e) to their respective complexes 7, 8, and 9 (Fig. 3b,d,f). The increase of electronegativity and electropositivity of oxygen and hydrogen atoms, respectively, were found from free L-his molecule 5 (Fig. 1b) to complexes 7, 8 and 9. It is obvious that the oxygen atoms due to the lack of charges attract charges from hydrogen atom, become more electronegative and thus leaves hydrogen atoms more electropositive, which results in a hydrogen bonding interaction. It is worthwhile to mention here that the presence of proton acceptor as well as donor oxygen in 7, 8 and 9 result in hydrogen bonding forces of interactions. The localization of electrostatic potential changed in good agreement with atomic charges that is increase in electronegativity of atoms decrease their electrostatic potential.

The common feature of intermolecular interaction between fullerenes 1, 2, 3 and 4 with L-his 5 is the

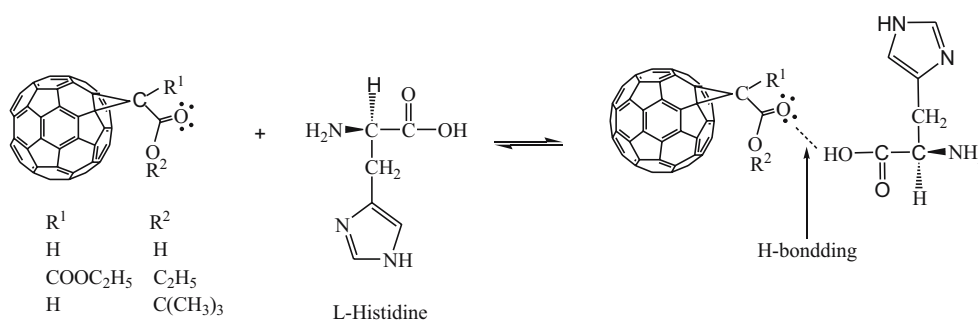
decrease in total energy of their respective complexes 6, 7, 8 and 9 as summarized in Table 2. It has been observed experimentally that fullerene and its derivative depict interaction with L-his, it is possible to gain of 547.1 hartrees corresponding to the addition of L-his molecule. This is a regular situation because there are reported Hartree-Fock energies for atoms, where it has been observed that energy diminishes when the number of atoms increases. [26]

The binding energy of fullerene  $C_{60}$ (1) with L-his (5), 391.01 kcal mol<sup>-1</sup> is calculated as the energy difference between the total energy of the 6 and the sum of the total energies of 1 and 5. Similarly, 1023.9 kcal mol<sup>-1</sup>, 1036.1 kcal mol<sup>-1</sup> and 1022.3 kcal mol<sup>-1</sup> are the values of the binding energy of fullerene derivatives 2, 3 and 4 with L-his, respectively. Thus, the complex 8 formed between diethyl (1,2-methanofullerene  $C_{60}$ )-61-61-dicarboxylate 3 and L-his 5 is more stable than complexes 6, 7 and 9. Thus, the obtained theoretical data are in quite good agreement with the experimental results, since diethyl (1,2-methanofullerene  $C_{60}$ )-61-61-dicarboxylate has been reported previously as the best and stable electrode for enantioanalysis of L-histidine than other fullerenes 1, 2 and 4.

LUMO and LUMO+1 of all the compounds along 1 to 9 have higher in energy than their respective HOMO and HOMO-1. Accordingly, the Fukui postulate [27] is fulfilled since electrons in orbital with higher energy are more susceptible to receive the nucleophilic species, whereas the electrons in orbital with lower energy are more susceptible to receive the electrophilic species.

Dipole moments ( $\mu$ ) as shown in Fig. 4, of the complexes 6, 7, 8 and 9 are greater than their respective fullerenes 1, 2, 3 and 4 as the addition of polar L-his 5 modifies the charge distribution in the complexes. Fullerene derivatives 2, 3 and 4 have higher dipole moment than  $C_{60}$  fullerene 1, probably because of the presence of bridge carbon atom C61 and functional group attached to it increase their polarity.  $C_{60}$  fullerene double bonds have polarization in opposite direction of its other double bonds that nullifies the electronic density of  $C_{60}$  and thus has the zero dipole moment.

**Scheme 1** Complexation of L-histidine with  $C_{60}$  fullerene derivatives



It is observed that the hardness values clearly indicate that the molecule 5 (L-his) is harder than all the other molecules, however on interaction with 1, 2, 3 and 4 slightly increases the hardness values of its respective complexes 6, 7, 8 and 9 (Fig. 5). Thus, this property supports the fact that according to Pearson [28] the soft molecules are more reactive than the hard molecules.

Computing their harmonic normal modes of vibration assessed the structural stability and feasibility of all the molecules 1 to 9. The lowest-lying normal mode of vibration of each of the molecules 1 to 9 is of frequency at  $266.72\text{ cm}^{-1}$ ,  $14.00\text{ cm}^{-1}$ ,  $25.45\text{ cm}^{-1}$ ,  $24.68\text{ cm}^{-1}$ ,  $44.62\text{ cm}^{-1}$ ,  $90.11\text{ cm}^{-1}$ ,  $12.58\text{ cm}^{-1}$ ,  $12.47\text{ cm}^{-1}$  and  $14.59\text{ cm}^{-1}$ , respectively. The absence of imaginary frequencies indicates that the structures of the all molecules are local minima on the corresponding potential energy surfaces.

Successful rationalizations of enantioselectivity depend upon comprehensive knowledge about the reaction mechanism [29]. The complex formation mechanism for fullerene derivatives 2, 3 and 4 with L-his is demonstrated below in Scheme 1. The complex between 2 and L-his is a result of two intermolecular hydrogen bonding interactions. While the complex between 3 and 4 with L-his is a result of one intermolecular hydrogen bonding interaction.

The total energy, frontier orbital energies, hardness, dipole moment, atomic charges, intermolecular forces of interaction and bond length parameters, were helpful to provide a logical explanation of the nature in which the complexation between  $C_{60}$  fullerene and different fullerene derivatives with L-his occurs.

## Conclusion

Based on the obtained results from computational calculations; it is concluded that there is intermolecular forces of interaction implicated between L-histidine and native fullerene or/and different fullerene derivatives. The interactions between fullerene derivatives and L-histidine are the hydrogen bonding interactions. These computational and experimental results certainly promise the enantioselective application of fullerene and its derivatives for the analysis of L-histidine in pharmaceutical formulation.

**Acknowledgements** Dr. Lal gratefully acknowledge the financial support from National Research Foundation, South Africa.

## References

1. Aboul-Enein HY, Wainer IW (1997) The impact of stereochemistry on drug development and use. Wiley, New York
2. Stone AJ (2002) The theory of intermolecular forces. Clarendon Press, Oxford
3. Rigby M, Smith EB, Wakeham WA, Maitland GC (1986) The forces between molecules. Oxford Science, Clarendon Press, Oxford
4. Kroto HW, Heath SC, O'Brien RF, Smalley RE (1985) Nature 318:162–163
5. Wilson SR (2002) Nanomedicine: Fullerene and carbon nanotube biology. In: E Osawa (ed) Kluwer, Dordrecht
6. Schinazi RF, Chiang LY, Wilson LJ, Cagle DW, Kadish KM, Ruoff RS (ed.) (1997) Fullerenes: Recent advances in the chemistry and physics of fullerenes and related materials, vol. 4, The Electrochemical Society, Pennington, NJ, pp 357–360
7. Friedman SH, Ganapathi PS, Rubin Y, Kenyon GL (1998) J Med Chem 41:2424–2429
8. Schuster DI, Wilson SR, Schinazi RF (1996) Bioorg Med Chem Lett 6:1253–1256
9. Friedman SH, DeCamp DL, Sijbesma RP, Srdanov G, Wudl F, Kenyon GLJ (1993) J Am Chem Soc 115:6506–6509
10. Dugan LL, Gabrielsen JK, Yu SP, Lin TS, Choi DW (1996) Neurobiol Disease 3:129–135
11. Tokuyama H, Yamago S, Nakamura E, Shiraki T, Sugiura Y (1993) J Am Chem Soc 115:7918–7919
12. Chen HHC, Yu C, Ueng TH, Chen S, Chen BJ, Huang KJ, Chiang LY (1998) Toxicol Pathol 26:143–151
13. Braden BC, Goldbaum FA, Chen BX, Kirschner AN, Wilson SR, Erlanger BF (2000) Proc Natl Acad Sci, USA, 97:12193–12197
14. Stefan-van Staden R-I, Lal B (2006) Anal Lett 39:1311–1319
15. Cioslowski J (1999) Electronic structure calculations on fullerenes and their derivatives. Oxford University Press
16. Wagner A, Flaig R, Zobel D, Dittrich B, Bombicz P, Strumpel M, Luger P, Koritsanszky T, Krane HG (2002) J Phys Chem A 106: 6581–6590
17. Slanina Z, Rudzinski T, Osawa E (1987) Collect Czech Chem Commun 52:2831
18. For yearly progress reports see: Fullerene, Proc. Electrochem. Soc. 1994–2001, 1–11, Electrochemical Society, Pennington, NJ, USA
19. Beck MT (1998) Pure Appl Chem 70:1881–1887
20. Bhattacharya S, Bauri AK, Chattopadhyay S, Banerjee M (2005) J Phys Chem B 109:7182–7187
21. Borowicz KK, Swiader M, Kaminski R, Kuzniar H, Kleinrok Z, Czuczwar SJ (2000) Pol J Pharmacol 52:345–352
22. Harris CI, Milne G (1981) British J Nutrit 45:423–429
23. Stefan-van Staden R-I, Lal B, Holo L (2006) Talanta in Press
24. Spartan'04 Version 1.0.3, Wavefunction, Inc, Irvine, CA
25. Kratschmer W, Lamb LD, Fostiropoulos K, Huffman DR (1990) Nature 347:354–358
26. Gadre SR, Sears SB, Chakravorty SJ, Bengale RD (1985) Phys Rev A32:2602–2606
27. Fukui K (1982) Science 218:747–754
28. Pearson RG (1987) J Chem Edu 64:561–567
29. Brandt P, Hedberg C, Lawonn K, Pinho P, Andersson PG (1999) Chem Eur J 5:1692–1699